The Interfacial Properties of Ferrosoferric Oxide in Aqueous Potassium Nitrate Solution

Kyoo Shik Shim, Taikyue Ree*

Pacific Chemical Ind. Co., Ltd., R & D Center

* Department of Chemistry, Korea Advanced Institute of Science and Technology

ABSTRACT

The interfacial properties of ferrosoferric oxide suspended in aqueous KNO_3 solution are investigated by studying the zeta potentials and surface charge densities at 25°C. The zeta potentials are obtained by measuring the electrophoretic mobility and the surface charge densities by potentiometric titrations in the aqueous KNO_3 solutions of different concentrations from 10^{-3} to 10^{-1}M. The data are interpreted by the surface dissociation and complexation model of Davis, et als. and the modified model.

1. INTRODUCTION

Metal oxides is one of the largest components of pigments used as coloring material. Dispersion stability is determined by the chemical interactions of vehicle with the pigmentary particles.[1] The chemical interactions between the metal oxides and simple ions, surfactants, polyelectrolytes, or polymers in vehicle control the stabilization of pigments because they control the surface charges in the media. Interfacial studies of oxides were performed through the adsorption measurements, potentiometric titrations, or electrokinetic measurements. Oxide/electrolyte interfacial systems behave in a different way than the classical ones, such as Hg/electrolyte and AgI/electrolyte electrode. Many models have been proposed for the oxide systems,[2-4] but they could not explain all the experimental data completely. Nowadays modified site-binding models have been often used for describing the electrical double layer (EDL) phenomena of metallic oxides.[5-10] Sprycha modified the model of Davis, James, and Leckie (DJL) more elaborately, and explained the results

of the potentiometric titrations, adsorption measurements and electrokinetic measurements in electrolyte solution. [11, 12]

In our work, Fe_3O_4/electrolyte-solution system has been studied by potentiometric titrations and electrophoretic mobility measurements. We used simplified assumptions to determine the acidity constants and complexation constants.

2. ELECTRICAL DOUBLE LAYER MODEL OF OXIDES

In the presence of water, metal oxides are covered with surface hydroxyl groups. A hydroxylated oxide particle can be understood as a polymeric oxoacid or -base. Figure 1 shows the cross sections of the surface layer of a metal oxide. [13] The formation of surface charge results from the following reactions; [5]

$$SOH_2^+ \overset{K_{a1}^{int}}{\rightleftharpoons} SOH + H_s^+ \tag{1}$$

$$SOH \overset{K_{a2}^{int}}{\rightleftharpoons} SO^- + H_s^+ \tag{2}$$

$$SOH + K_s^+ \overset{{}^*K_{K^+}^{int}}{\rightleftharpoons} SO^- \cdot K^+ + H_s^+ \tag{3}$$

$$SOH_2^+ \cdot NO_3^- \overset{{}^*K_{NO_3}^{int}}{\rightleftharpoons} SOH + H_s^+ + NO_3^- \; s \tag{4}$$

where S indicates surface of Fe_3O_4, s denotes the surface to which H^+, K^+ and NO_3^- attached and the equilibrium constants K's are expressed by the following equations;

$$K_{a1}^{int} = \frac{[SOH][H^+]}{[SOH_2^+]} \cdot \exp\left(\frac{-e\,\psi_o}{kT}\right) \tag{5}$$

$$K_{a2}^{int} = \frac{[SO^-][H^+]}{[SOH]} \cdot \exp\left(\frac{-e\,\psi_o}{kT}\right) \tag{6}$$

$${}^*K_{K^+}^{int} = \frac{[SO^-K^+][H^+]}{[SOH][K^+]} \cdot \exp\left(\frac{-e(\psi_o-\psi_\beta)}{kT}\right) \tag{7}$$

$${}^*K_{NO_3}^{int} = \frac{[SOH][H^+][NO_3^-]}{[SOH_2^+ \cdot NO_3^-]} \cdot \exp\left(\frac{-e(\psi_o-\psi_\beta)}{kT}\right) \tag{8}$$

$$[H^+]_s = [H^+] \cdot \exp\left(\frac{-e\,\psi_o}{kT}\right) \tag{9}$$

where the superscript int indicates "intrinsic", ψ_o and ψ_β are the surface potential and the inner Stern plane potential, respectively, and K with the asterisk denotes for the equilibrium constant for the complexes $SO^- \cdot K^+$ and $SOH_2^+ \cdot NO_3^-$.

From the above explanation, the model of electrical double layer can be pictured in Fig. 2. The surface charge density σ_o, as measured by potentiometric titration, is then given by ;

$$\sigma_o = B([SOH_2^-] + [SOH_2^+ \cdot NO_3^+] - [SO^-] - [SO^- \cdot K^+]) \quad (10)$$

whereas the inner Stern plane-surface-charge (σ_β) is:

$$-\sigma_\beta = B([SOH_2^+ \cdot NO_3^-] - [SO^- \cdot K^+]) \quad (11)$$

and the diffuse layer charge (σ_d), calculated from the ζ-potential, is;[14]

$$-\sigma_d = B([SOH_2^+] - [SO^-]) \quad (12)$$

$$= +11.74\sqrt{C}\sinh(19.46Z\psi_d) \quad (13)$$

The electroneutrality[15] reguires that

$$\sigma_o + \sigma_\alpha + \sigma_d = 0 \quad (14)$$

The surface site density N_S is ;

$$N_S = B([SOH_2^+] + [SOH_2^+ \cdot NO_3^-] + [SO^-] + [SO^- \cdot K^+] + [SOH]) \quad (15)$$

At pH pH_o, pH_o is the pH at the point of zero charge, $[SOH_2^+]$ is much larger than $[SO^-]$, and $[SOH_2^+ \cdot NO_3^-]$ is larger than $[SO^- \cdot K^+]$. Then from eqs. (10), (11), (12) and (15), the following equations follow;

$$\sigma_o = B([SOH_2^+] + [SOH_2^+ \cdot NO_3^-]) \quad (16)$$

$$-\sigma_\beta = B[SOH_2^+ \cdot NO_3^-] \quad (17)$$

$$-\sigma_d = B[SOH_2^+] \quad (18)$$

and

$$N_S = B([SOH_2^+] + [SOH_2^+ \cdot NO_3^-] + [SOH]). \quad (19)$$

From eqs. (5) and (8) and by using eqs (16)–(19), the following relationships are obtained;

$$pK_{a1}^{int} = pH + \log\left(\frac{|\sigma_d|}{N_s - \sigma_o}\right) + \frac{e\psi_o}{2.3kT} \tag{20}$$

$$= pQ_{a1} + \frac{e\psi_o}{2.3kT} \tag{21}$$

$$\text{where } pQ_{a1} = pH + \log\left(\frac{|\sigma_d|}{N_s - \sigma_o}\right) \tag{21a}$$

$$^{*}pK_{NO_3}^{int} = pH + \log\left(\frac{\sigma_o + \sigma_d}{N_s - \sigma_o}\right) - \log[NO_3^-] + \frac{e(\psi_o - \psi_\beta)}{2.3kT} \tag{22}$$

$$= p^*Q_{NO_3} + \frac{e(\psi_o - \psi_\beta)}{2.3kT} \tag{23}$$

$$\text{where } p^*Q_{NO_3} = pH + \log\left(\frac{\sigma_o + \sigma_d}{N_s - \sigma_o}\right) - \log[NO_3^-] \tag{23a}$$

By the same method, when $pH > pH_0$ $[SO^-]$ is much larger than $[SOH_2^+]$, so that $[SO^- \cdot K^+]$ is larger than $[SOH_2^+ \cdot NO_3^-]$. Then from eqs. (10), (11), (12) and (15), the following equations result;

$$-\sigma_o = B([SO^-] + [SO^- \cdot K^+]) \tag{24}$$

$$\sigma_\beta = B[SO^- \cdot K^+] \tag{25}$$

$$\sigma_d = B[SO^-] \tag{26}$$

and

$$N_s = B([SO^-] + [SO^- \cdot K^+] + [SOH]) \tag{27}$$

from eqs (6) and (7) and by using eqs. (24)-(27) the following relationships are obtained;

$$pK_{a2}^{int} = pH - \log\left(\frac{\sigma_d}{N_s - |\sigma_d|}\right) + \frac{e\psi_o}{2.3kT} \tag{28}$$

$$= pQ_{a2} + \frac{e\psi_o}{2.3kT} \tag{29}$$

$$\text{where } pQ_{a2} = pH - \log\left(\frac{\sigma_d}{N_s - |\sigma_d|}\right) \tag{29a}$$

$$p^*K_{K^+}^{int} = pH - \log\left(\frac{|\sigma_o + \sigma_d|}{N_s - |\sigma_d|}\right) + \log[K^+] \tag{30}$$

$$+ \frac{e(\psi_o - \psi_\beta)}{2.3kT} = p^*Q_{K^+} + \frac{e(\psi_o - \psi_\beta)}{2.3kT} \tag{31}$$

$$\text{where } p^*Q_{K^+} = pH - \log\left(\frac{|\sigma_o + \sigma_d|}{N_s - |\sigma_d|}\right) + \log[K^+] \tag{31a}$$

Because surface potential ψ_o is zero at point of zero charge pH_o, from eq. (21), the following relation results;

$$pK_{a1}^{int} = pQ_{a1}$$

similarly $$pK_{a2}^{int} = pQ_{a2}$$

in the above pQ_{a1} and pQ_{a2} are obtained experimentally as will be mentioned later. Thus pK_{a1}^{int}, and $p^*K_{a2}^{int}$ are obtained. By a same procedure, $p^*K_{k+}^{int}$ and $p^*K_{NO_3^-}$ are obtained from the experimental values of p^*Q_{k+} and $p^*Q_{NO_3^-}$ since $\psi_o = \psi_\beta$ at pH_o. [see eq 23].

3. EXPERIMENTAL

1) Materials

Fe_3O_4 is a commercially available compound manufactured by Sun Chemical, USA. The black iron oxide was pulverized three times, and washed by hot water until the specific conductance of the supernatant is less than 0.5 $\mu\Omega^{-1}$ cm^{-1}, and then dried at 80°C in a vacuum oven. The specific surface area was determined by the BET method, and the value was $3.87 m^2 g^{-1}$. Extra pure Potassium nitrate (Junsei, Japan) was recristalized from water. The water used in this work was purified by an ion exchange and then by distillation. Nitric acid and possium nitrate were the analytical reagent grade (Malmcrodt, USA).

2) Surface Charge Measurements

The measurements were performed by a potentiometric titration of an aqueous suspension of Fe_3O_4 in an aqueous KNO_3 solution (10^{-3}, 10^{-2}, 10^{-1}M) at 25±0.5°C. As the titrant, a 0.01M solution of KOH was used. The alkaline solution was stored in polyethylene bottle to avoid silicate contamination.

The titration cell[16] was a flat-bottomed 500ml beaker with a rubber stoper through which passed the electrodes, a thermometer, a 10ml buret, and an inlet and outlet for purified nitrogen gas, which was used to drive off the oxygen and CO_2 dissolved in the solution and also to make the nitrogen atmosphere of

the cell. The suspension was continuously stirred by a tefloncovered magnetic stirrer. Purified N_2 was passed through the solution before and during the experiment. The experimental procedure was a s follows: 5g Fe_3O_4 was suspended in 250ml of solution containing KNO_3 of appropriate concentration, and pH was adjusted to 4 using 0.01M HNO^3 solution. And then the suspension was titrated by using KOH solution of 10^{-2}M. This procedure was also carried out for blank solution, not including Fe_3O_4.

3) Electrophoretic mobility Measurements.

These were carried out using a Laser Zee Meter Model 501 (Pen Kem Company, USA), which includes a microelectrophoretic cell of rectangular cross section.[17] Fe_3O_4 was suspended in 10^{-3}M KNO_3. Purified nitrogen gas was passed through the suspension before measurements. Mobility measurements were performed between pH 4 and 10 at room temperature, and these values were corrected to 25°C by using a manual table.

4. RESULTS AND DISCUSSION

The surface charge density (σ_o , μC cm^{-2}) on Fe_3O_4 can be determined by potentiometric titrations and calculations from the following equation.[14]

$$\sigma_o = F(\Gamma_{H^+} - \Gamma_{OH^-})$$

where F is the Faraday constant ($Cmole^{-1}$), Γ_{H^+} and Γ_{OH^-} are thesurface excess concentration (mole cm^{-2}) of the potential determining ions H^+ and OH^-, respectively. The dependence of surface charge on the pH of KNO_3 solutions is presented in Fig. 3. From Fig. 3, the point of zero charge (pH_o) for Fe_3O_4 is at pH 6.8. The electrophoretic mobility μ vs. pH curve is shown in Fig.4. The ζ -potential was calculated from the electrophoretic mobility data according to Wiersema et als,[18] and the average particle diameter of Fe_3O_4 was calculated from the BET surface area as 0.31μm. The diffuse layer charge density (σ_d) was obtained from the -potential by the Gouy-chapman equation. The surface charge density and electrophoretic mobility data are listed in Table I.

In Table II our experimental values of pQ_{a1} and pQ_{a2} are summarized in various pH and 10^{-3}M KNO_3 solution, where pQ_{a1} expresses the values when pH

$<pH_o$ while pQ_{a2} indicates those at $pH > pH_o$. pQ_{a1} is evaluated from eq. (21a) by using the experimental values of σ_o and σ_d in Table I, the surface site density N_s being taken as $N_s = 6nm^{-2}$ (= 96.12 $\mu C\ cm^{-2}$).[9] In Fig.s 5 and 6 pQ_{a1} and pQ_{a2} are plotted against α (= $|\sigma_o|/N_s$), respectively. We see that the linearity between pQ_{a1} and α is good. The reason is following; In eq. (21a), the term $\log |\sigma_d| /(N_s - \sigma_o)$ transforms in the following way;

$$\log\left(\frac{|\sigma_o|}{N_s - \sigma_o}\right) = \log\left(\frac{\alpha}{1-\alpha}\ \frac{|\sigma_d|}{\sigma_o}\right)$$

The quantity $|\sigma_d/\sigma_o|$ is about constant according to our experimental results. Thus

$$PQ_{a1} = pH + \log\left(\frac{\alpha}{1-\alpha}\right) + \log\left(\frac{|\sigma_d|}{\sigma_o}\right)$$

$$= PQ'_{a1} + \log\left(\frac{|\sigma_d|}{\sigma_o}\right) \qquad (32)$$

where $$PQ'_{a1} = pH + \log\left(\frac{\sigma_o}{N_s - \sigma_o}\right)$$

$$= pH + \log\left(\frac{\alpha}{1-\alpha}\right) \qquad (33)$$

According to DJL, pQ'_{a1} is proportional to α . Thus the linearity of pQ_{a1} vs. α is explained. In a similar way the experimental results shown in Fig. 6 is explained where pQ_{a2} is expressed by eq. (29a), from which the following equation is derived;

$$PQ_{a2} = pH - \log\left(\frac{\alpha}{1-\alpha}\right) - \log\left(\frac{\sigma_d}{|\sigma_o|}\right)$$

$$= pQ'_{a2} - \log\left(\frac{\sigma_d}{|\sigma_o|}\right) \qquad (34)$$

where $$PQ'_{a2} = pH - \log\left(\frac{|\sigma_o|}{N_s - |\sigma_o|}\right)$$

$$= pH - \log\left(\frac{\alpha}{1-\alpha}\right) \qquad (35)$$

The primed quantities in eqs (33) and (35) are defined by DJL. In Figs. 7 and 8 $^{*}pQ_{NO_3^-}$ and $^{*}pQ_{K^+}$ are plotted against α respectively, where $^{*}pQ_{NO_3^-}$ and $^{*}pQ_K^+$ are expressed (23a) and (31a). In our experiment the solution of KNO_3 (10^{-3}) was used, thus the terms $\log [NO_3^-]$ and $\log [K^+]$ in eqs. (23a) and (31a) turn to -3 and $+3$, respectively. Equation (23a) is transformed to the following form:

$$p^*Q_{NO_3^-} = pH + \log\left(\frac{\alpha}{1-\alpha}\right) - \log\left[NO_3^-\right] + \log\left(\frac{\sigma_o + \sigma_d}{\sigma_o}\right) \qquad (36)$$
$$= p^*Q'_{NO_3^-} + \log\left(\frac{\sigma_o + \sigma_d}{\sigma_o}\right)$$

Similarly eq. (31a) yields

$$p^*Q_{K^+} = pH - \log\left(\frac{\alpha}{1-\alpha}\right) + \log\left[K^+\right] - \log\left(\frac{|\sigma_o + \sigma_d|}{|\sigma_o|}\right)$$
$$= p^*Q_{K^+} - \log\left(\frac{|\sigma_o + \sigma_d|}{|\sigma_o|}\right)$$

The term log ($|\sigma_o + \sigma_d| / |\sigma_o|$) is very small quantity judged from the experimental data of σ_o and σ_d . Thus the following relation results:

$$p^*Q_{K^+} = p^*Q'^{+}_{K} \quad \text{and} \quad p^*Q_{NO_3^-} = p^*Q'_{NO_3^-}$$

In Table III $p^*K^{int}_{NO_3^-}$ and $p^*K^{int}_{K^+}$ are obtained from the $p^*Q_{NO_3^-}$ and $p^*Q_{K^+}$ values by an extrapolation to $\alpha = 0$. Thus or values of $p^*K^{int}_{NO_3^-}$ and $p^*K^{int}_{K}$ are equal to the primed quantities (DJL) by the relation of eq (38). In fact this relation is found in Table III.

Our data of pQ'_{a1} and pQ'_{a2} obtained in various concentrations of KNO_3 solution are summarized in Table IV. The pQ'_{a1} and pQ'_{a2} are plotted against α in Figs. 9 and 10. Note that DJL defined pQ'_{a1} and pQ'_{a2} by eqs. (33) and (35). That is, DJL substituted σ_o for σ_d in our equations (21a) and (29a). Although this substitution is problematic, we shall use temporarily the DJL methods in analyzing the results shown in Figs. 9 and 10. From the intercepts of the straight lines on the y-axis the pK^{int}_{a1} and pK^{int}_{a2} values are obtained. We compare the values of pK^{int}_{a1} and pK^{int}_{a2} at 10^{-3}M of KNO_3 with ours (unprimed) in the following;

pK^{int}_{a1} = 4.8M $\qquad$ pK^{int}_{a2} = 8.8M

pK^{int}_{a1} = 3.6M $\qquad$ pK^{int}_{a2} = 10.0M

The difference between (pK^{int}_{a1}) and pK^{int}_{a1} is understood from eqs. (33) and (32), i.e the term log ($|\sigma_d| / \sigma_o$) is omitted in the former; the difference in (pK^{int}_{a2}) and pK^{int}_{a2} is similar, i.e. by the term -log ($|\sigma_d / |\sigma_o|$) where

$|\sigma_d|/\sigma_o < 1$. We consider the difference between our model of the EDL and that of DJL's. Returning to Fig. 2 which represent the EDL model, we fond that DJL neglects the contribution of the surface complexes, $[SOH_2^+ \cdot NO_3^-]$ and $[SO^- \cdot K^+]$ in the development of surface charge. That is, the term $[SOH_2^+ \cdot NO_3^-]$ in eq. (16) is neglected in the DJL's model assuming that σ_o is due to only $[SOH_2^+]$ in dilute electralyte. This is not true: we believe that our model accords well with the real situation.

5. CONCLUSION

The surface charge increases and the mobility decreases with increasing electrolyte concentrations at a given pH. The overestimation of surface ionization at theinterface of Fe_3O_4/electrolyte-solution in the DJL's model makes K_{a1}^{int} smaller and K_{a2}^{int} larger than those in our model. The surface complexation plays a major role on the development of surface charge from the expermental resutls.

REFERENCES

1. Parfitt, G.D. (Ed.), "Dispersion of Powders in Liquids, "3rd Ed., Applied Science Puolishers, Englewood, NJ, (1981).
2. Healy, T.W. and White, L.R., Adv. Colloid & Interfaces Sci. *9,* 303 (1978).
3. Yates, D.E., Levine, S., and Healy, T.W., J. Chem. Soc. Faraday I., *70,* 1807 (1974).
4. Breeuwsma, A., and Lyklema, J., Disc. Faraday Soc. *52,* 324 (1971).
5. Davis, J.A., James, R.O., and Leckie, J.O., J. Colloid Interface Sci., *63,* 480 (1978).
6. Davis, J.A., and Leckie, J.O.J. Colloid Interface Sci., *67,* 90 (1978).
7. Davis, J.A., and Leckie, J.O.J. Colloid Interface Sci., *74,* 32 (1980).
8. Sposito, G., J. Colloid Interface Sci., *91,* 329 (1983).
9. Regazzoni, A.E., Blesa, M.A., and Maroto, A.J.G., J. Colloid Interface Sci., *91,* 560 (1983).
10. Sharma, M., and Yen, T.H., J. Colloid Interface Sci., *98,* 39 (1984).
11. Sprycha, R., J. Colloid Interface Sci., *102,* 173 (1984).
12. Sprycha, R., J. Colloid Interface Sci., *96,* 551 (1983).
13. Stumm, W., and Morgan, J.J., "Aquatic Chemistry", 2nd Ed., Wiley-

Interscience Publication, New York (1981).
14. Hunter, R.J., "Zeta Potential in Colloid Science", Academic Press Inc., London (1981).
15. Foissy, A., M'Pandou, A., and Lamarche, J.M., Colloids & Surfaces *5*, 363 (1982).
16. Parks, G.A., and de Bruyn, P.L., J. Phys. Chem. *66*, 967 (1962).
17. Goetz, P.J., and Penniman, J.G., American Laboratory, Oct. (1976); Pressented at the 49th National Colloid Symposium, June. 1975.
18. Wiersema, P.H., Loeb, A.L., and Overbeek, J. Th. G., J. Colloid Interface Sci., *22*, 78 (1966).

Table I. Surface Charge Density and Electropheretic Mobility Data in the Interface $Fe_3O_4/10^{-3}M\ KNO_3$.

pH	σ_o ($\mu C\ cm^{-2}$)	μ ($10^{-8}m^2V^{-1}S^{-1}$)	ζ (mV)	$-\sigma_d$ ($\mu C\ cm^{-2}$)
4.3	13.00	3.40	49.32	0.41
4.7	10.45	2.96	42.65	0.34
5.2	6.54	2.40	34.43	0.27
5.8	3.50	1.63	23.12	0.17
6.3	2.07	0.89	12.59	0.09
6.7	0.50	0.19	2.57	0.02
7.2	− 1.78	− 0.85	− 11.57	− 0.08
7.8	− 4.27	− 2.12	− 30.31	− 0.23
8.3	− 7.48	− 3.15	− 45.99	− 0.38
8.7	− 9.75	− 3.82	− 57.55	− 0.51
9.3	− 13.50	− 4.63	− 72.18	− 0.71

Table II. Aparent acidity constants, pQ_{a1} and pQ_{a2} of Fe_3O_4 in 10^{-3}M KNO_3 solution.

pH	pQ_{a1}	pH	pQ_{a2}
4.3	1.99	7.2	10.27
4.7	2.30	7.8	10.40
5.2	2.68	8.3	10.67
5.8	3.06	8.7	10.92
6.3	3.28	9.3	11.34

Table III. Comparison of interfacial parameters for Fe_3O_4 in 10^{-3}M KNO_3 solution obtained for our model and for DJL's model.

	ref. (9)*		this work	
	ours	DJL	ours	DJL
pK_{a1}^{int}	3.6	4.4	3.6	4.8
pK_{a2}^{int}	10.2	9.0	10.0	8.8
$^{*}pK_{k+}^{int}$	6.2	6.2	5.8	5.8
$^{*}pK_{NO_3}^{int}$	7.4	7.4	7.8	7.8

* The experimental data from Regazzoni et als. [9]

Table IV. Apparent acidity constants, pQ'_{a1} and pQ'_{a2} of Fe_3O_4 in 10^{-1}, 10^{-2} and 10^{-3}M KNO_3 solution

pH	pQ'_{a1}			pH	pQ'_{a2}		
	10^{-1}	10^{-2}	10^{-3}		10^{-1}	10^{-2}	10^{-3}
4.3	3.90	3.71	3.49	7.2	8.65	8.77	8.91
4.7	4.23	4.02	3.79	7.8	8.72	8.78	9.14
5.2	4.58	4.38	4.06	8.3	8.95	9.03	9.37
5.8	4.95	4.75	4.37	8.7	9.20	9.30	9.64
6.3	5.13	4.87	4.65	9.3	9.64	9.73	10.09

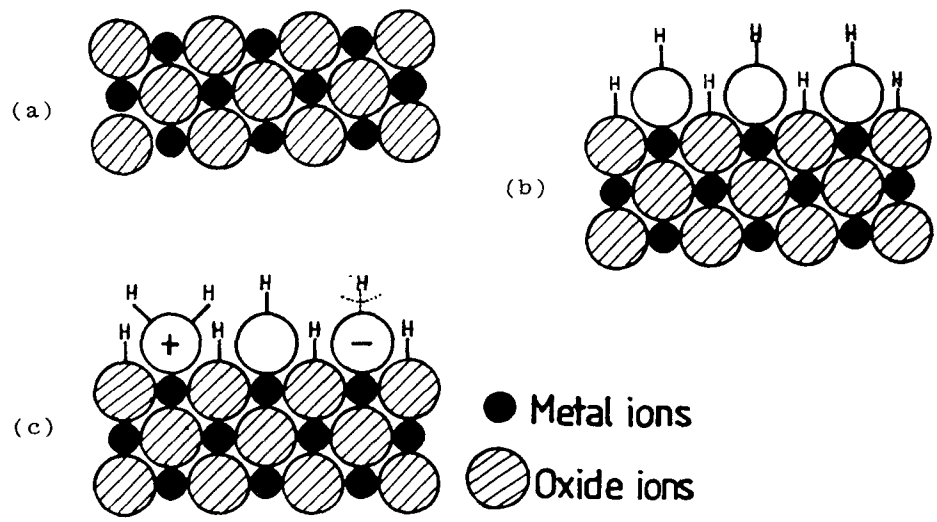

Fig. 1. Cross sections of the surface layer of a typical metal oxide. (a) The metal oxide surface. (b) The water molecules chemisorbed on the oxides surfaces. The open large circle carrying H indicates the OH group of the water molecule chemisorbed to the metallic ion, the other H atom of the water molecule being adsorbed to the neighboring oxide ion. (c) The coordination of H^+ ions to the surface and the dissociation of H atoms from the surface. The OH group on the surface shown in Fig. 1 (b) coordinates to it H^+ from the solution charging the oxygen atom positively while the H atom can be removed by a base from the surface charging the oxygen atom negatively.

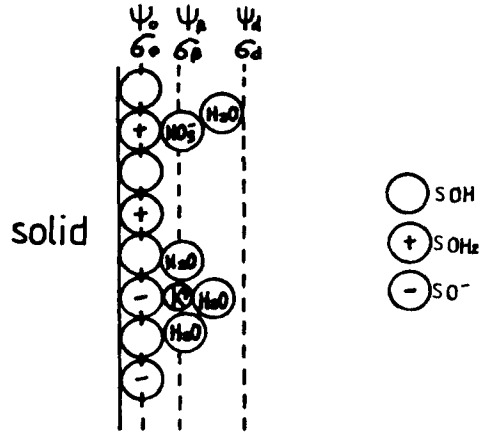

Fig. 2. Schematic representation of the double layer model showing the position of the surface charges and potentials. The double layer shows the surface shown in Fig. 1 (c). The S in SOH, SOH_2^+, SO^- indicate the surface to which OH, OH_2^+ and O^- are attached as shown in Fig. 1 (c).

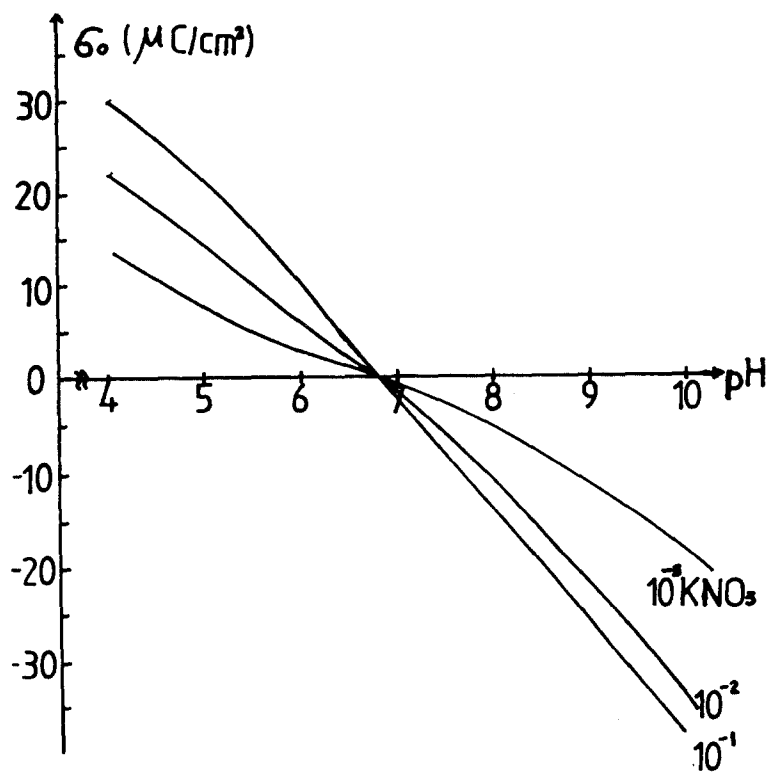

Fig. 3. Surface charge density of Fe_3O_4 as a function of pH in the presence of three different concentrations of KNO_3 at 25°C.

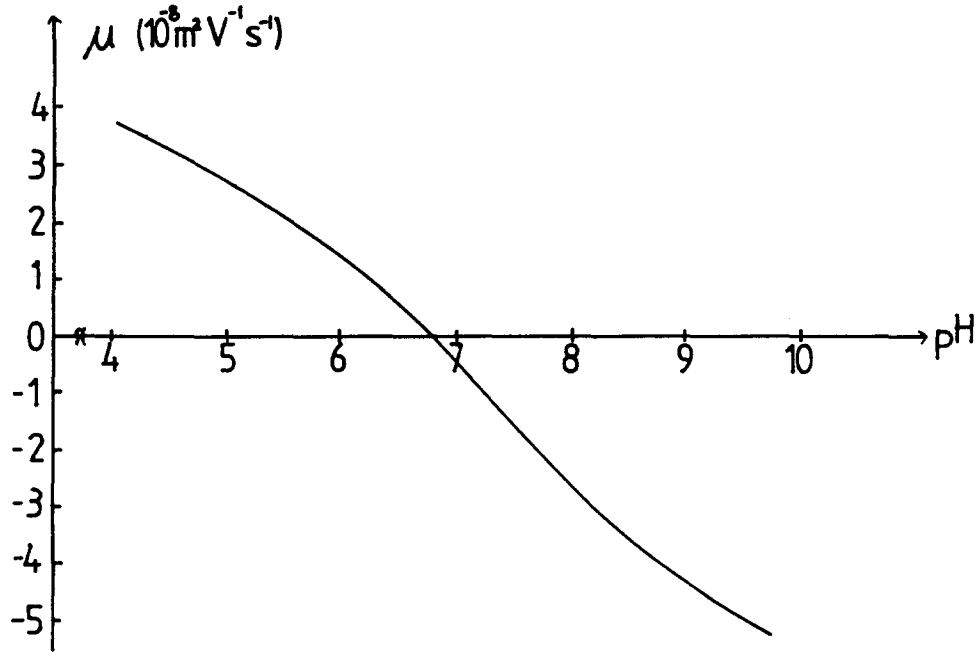

Fig. 4. Electrophoretic mobility of Fe_3O_4 as a function of pH in 10^{-3}M KNO_3 solution at 25°C.

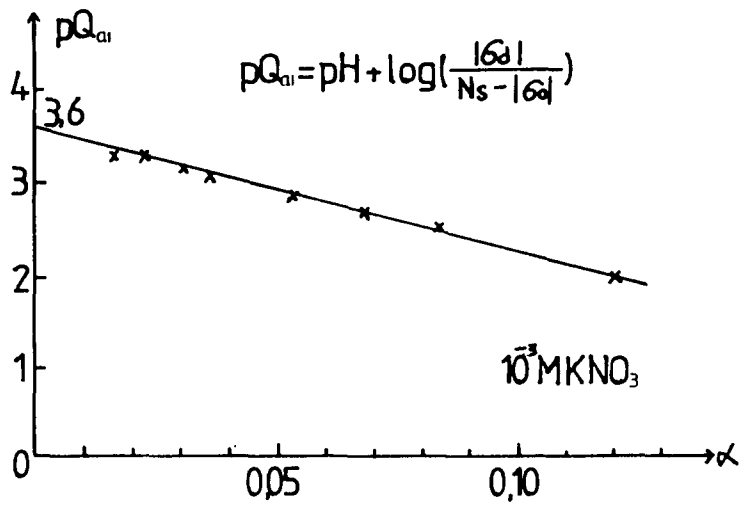

Fig. 5. Plot of pQ_{a1} calculated by using the modified model as a function of fractional reaction sites for Fe_3O_4 in 10^{-3}M KNO_3 solution.

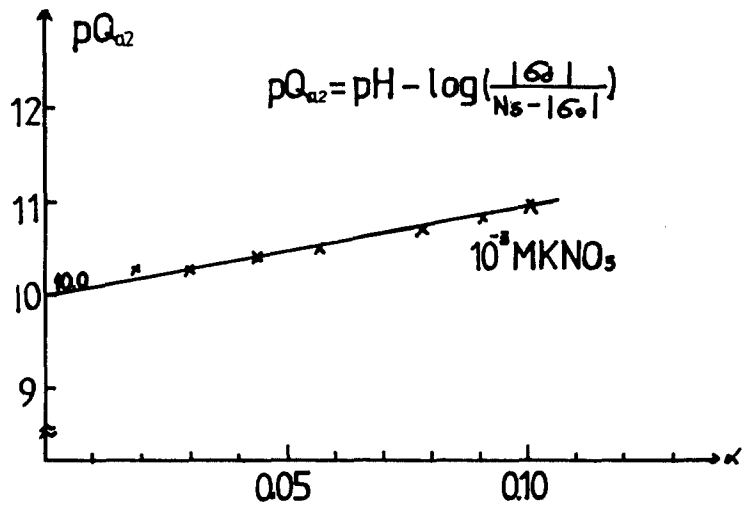

Fig. 6. Plot of pQ_{a2} calculated by using the modified model as a function of fractional reaction sites for Fe_3O_4 in 10^{-3}M KNO_3 solution.

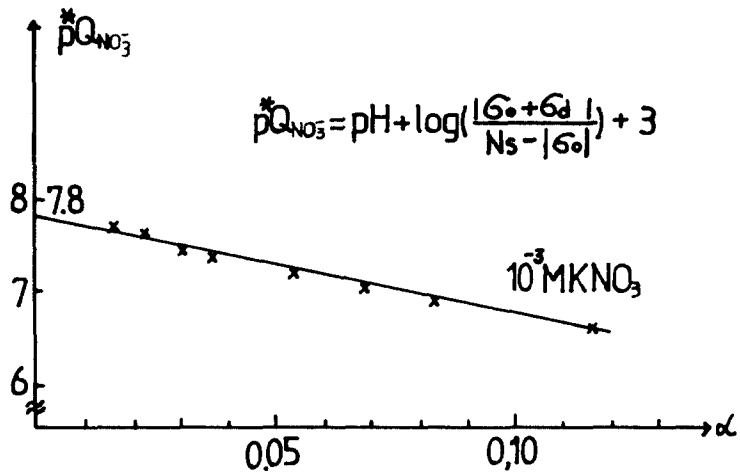

Fig. 7. Plot of $^{*}pQ_{NO_3}$ calcuated by using the modified model as a function of fractional reaction sites for Fe_3O_4 in 10^{-3}M KNO_3 solution.

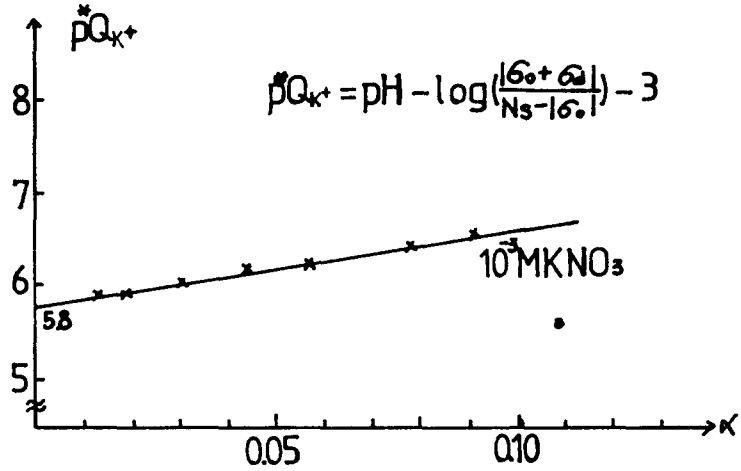

Fig. 8. Plot of $^{*}pQ_{K^+}$ calculated by using the modified model as a function of fractional reaction sites for Fe_3O_4 in 10^{-3}M KNO_3 solution.

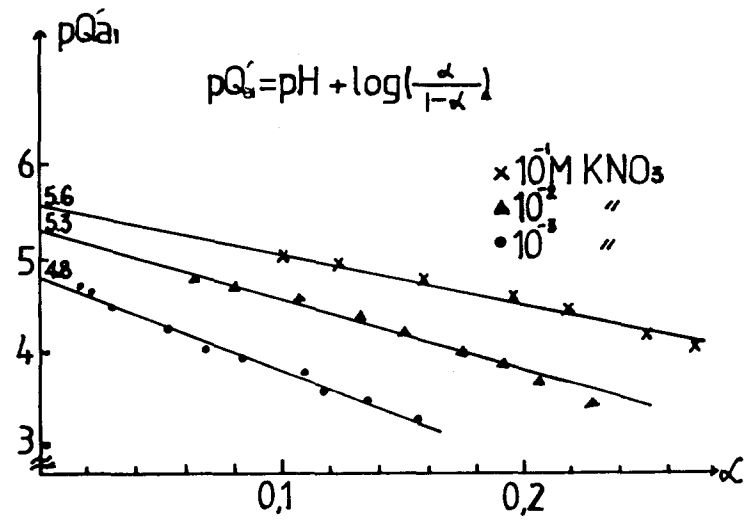

Fig. 9. Plot of pQ'_{a1} calcuated by using the DJL model as a function of fractional reaction sites for Fe_3O_4 in KNO_3 solution.

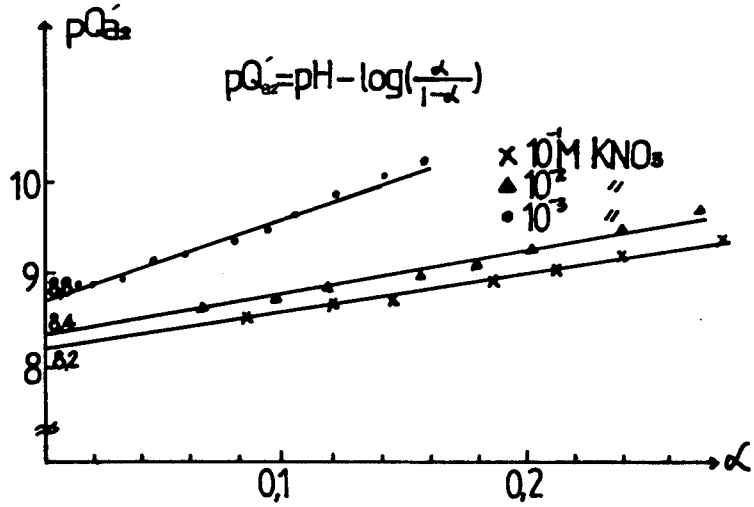

Fig. 10. Plot of pQ'_{a2} calculated by using the DJL model as a function of fractional reaction sites for Fe_3O_4 in KNO_3 solution.